Heat flux in chains of nonlocally coupled harmonic oscillators: Mean-field limit

Lucianno Defaveri [1,*] Carlos Olivares [1,2] and Celia Anteneodo [1,3]

[1]*Department of Physics, PUC-Rio, Rio de Janeiro, 22451-900 Rio de Janeiro, Brazil*

[2]*Laboratoire de physique de l'École normale supérieure (PSL University), CNRS, Sorbonne Université, and Université de Paris, 75005 Paris, France*

[3]*Institute of Science and Technology for Complex Systems, INCT-SC, Brazil*

(Received 9 November 2021; accepted 4 May 2022; published 26 May 2022)

We consider one-dimensional systems of all-to-all harmonically coupled particles with arbitrary masses, subject to two Langevin thermal baths. The couplings correspond to the mean-field limit of long-range interactions. Additionally, the particles can be subject to a harmonic on-site potential to break momentum conservation. Using the nonequilibrium Green's operator formalism, we calculate the transmittance, the heat flow, and local temperatures for arbitrary configurations of masses. For identical masses, we show analytically that the heat flux decays with the system size N as $1/N$ regardless of the conservation or not of the momentum and of the introduction or not of a Kac factor. These results describe, in good agreement, the thermal behavior of systems with small heterogeneity in the masses.

DOI: 10.1103/PhysRevE.105.054149

I. INTRODUCTION

Simplified microscopic models, such as classical particle chains in contact with heat baths, have proven useful to gain insights about the physics of thermal transport [1–4]. Especially, the role of conserved quantities in the violation of Fourier's law has been extensively studied [5–11]. Actually, the interest in one-dimensional models goes beyond the higher accessibility from a theoretical approach, as they can also be useful for understanding the heat conduction anomalies observed in real systems, such as carbon nanotubes [12], silicon nanowires [13], molecular chains [14,15], and others [16]. In particular, these experiments and theories can lead to new developments based on phonon transport, such as thermal diodes [17–20]. In this latter context, the range of interactions may be relevant to increase rectification [21,22]. More generally, sufficiently long range interactions are worth investigating as they can bring new physical features to a system [23–26]. Among them, let us cite negative specific heat [26], ensemble inequivalence [27], phase transitions even in one-dimensional systems [28–31], slow relaxation, and long-lived quasistationary states [32–36].

Despite the distinct role that the range of the interactions might play in heat transport, most studies rely on nearest-neighbor couplings. Recent works tackling long-range systems are based mainly on molecular dynamics simulations [37–45]. Variants of Fermi-Pasta-Ulam-Tsingou [39–42,45] and XY [37,40,43] chains, with interactions that decay algebraically with the interparticle distance, have been studied. But few analytical results exist for long-range systems in this context. Among them, let us note the contribution by Tamaki and Saito [46], who considered chains of long-range coupled harmonic oscillators with momentum exchange and studied the thermal properties through the Green-Kubo formula that relates the equilibrium energy current correlation function to the thermal conductivity. However, for sufficiently long range systems, the divergence of the current correlation hampers that calculation.

The infinite-range limit is an analytically tractable case that may allow us to gain insights about long-range systems. This limit for a network of harmonic oscillators, when springs are random, was previously tackled through a random matrix approach [47]. In the present work, we consider another variant of the globally coupled harmonic system, with identical couplings, and use the nonequilibrium Green's function formalism to calculate analytically the heat current J, via the transmittance, as a function of the system size N. In contrast to the well-known case of harmonic first-neighbor interactions, for which the heat current becomes constant for large N, we find that for the opposite extreme of infinite-range interactions, the current decays as $1/N$. This result also contrasts with that found when spring disorder is introduced [47].

In Sec. II, we describe the model system. Following the nonequilibrium Green's function approach, in Sec. III, we calculate the transmittance, heat flow, and local temperature, showing the behavior with system size, for different mass

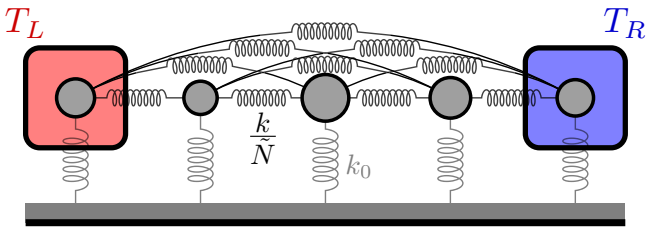

FIG. 1. Pictorial representation of the system.

[*]Present address: Department of Physics, Bar Ilan University, Ramat-Gan 52900, Israel.

distributions, and analytical results are shown for identical masses. Section IV contains final remarks about the scope of the results.

II. MODEL

We consider a system of N globally coupled harmonic oscillators described by the Hamiltonian

$$\mathcal{H} = \sum_{n=1}^{N} \frac{p_n^2}{2m_n} + \frac{k_0}{2}\sum_{n=1}^{N} q_n^2 + \frac{k}{2\tilde{N}}\sum_{n=1}^{N}\sum_{\substack{j=1\\ j\neq n}}^{N} \frac{1}{2}(q_n - q_j)^2, \quad (1)$$

where p_n and q_n are, respectively, the one-dimensional momentum and displacement of the nth oscillator with mass m_n, while k_0 and k are the stiffness constants of the pinning and the internal interactions, respectively, and $\tilde{N}$ is a factor that, when $\tilde{N} = N - 1$, represents the Kac factor [48], warranting extensivity in the thermodynamic limit, but $\tilde{N} = 1$ will also be considered for comparison with previous studies. This system is very similar to that studied by Schmidt *et al.* [47], but in that case spring constants are random, masses are equal, and a Kac factor is not used. The impact of these differences will be noted throughout this paper.

Notice that the last term of the Hamiltonian can be seen as the infinite-range limit of a chain of harmonic oscillators that interact with a strength that decays with distance between particles. In this limit, however, the spatial order of the chain is lost. A schematic representation of the system is given in Fig. 1.

Langevin thermostats are put in contact with two of the oscillators. Let us choose the first and Nth ones. The resulting equations of motion are

$$m_1\,\ddot{q}_1 = F_1 - \gamma\,\dot{q}_1 + \eta_L, \quad (2)$$

$$m_n\,\ddot{q}_n = F_n, \quad n \neq 1, N, \quad (3)$$

$$m_N\,\ddot{q}_N = F_N - \gamma\,\dot{q}_N + \eta_R, \quad (4)$$

where γ is the friction coefficient; $\eta_{L/R}$ are independent fluctuating zero-mean Gaussian forces, such that $\langle \eta_{L/R}(t)\,\eta_{L/R}(t')\rangle = 2\gamma T_{L/R}\,\delta(t-t')$ and $\langle \eta_L(t)\eta_R(t')\rangle = 0$; and the force over particle n is

$$F_n = -k_0\,q_n + \frac{k}{\tilde{N}}\sum_{\substack{j=1\\ j\neq n}}(q_j - q_n). \quad (5)$$

After Fourier transforming the equations of motion (2)–(4), through the definition $\hat{x}(\omega) = \int_{-\infty}^{\infty} x(t)e^{-i\omega t}dt$, in matrix form, they become

$$\hat{Z}(\omega)\hat{q}(\omega) = \hat{\eta}(\omega), \quad (6)$$

where $\hat{q}(\omega) = (\hat{q}_1(\omega), \ldots, \hat{q}_N(\omega))^T$ is the Fourier-transformed column vector of displacements, $\hat{\eta}(\omega) = (\eta_L(\omega), 0, \ldots, 0, \eta_R(\omega))^T$ is the noise column vector, and the $N \times N$ matrix $\hat{Z}(\omega)$ has the symmetric form

$$\hat{Z}(\omega) = \begin{pmatrix} a_1 + c & b & \cdots & b & b \\ b & a_2 & b & \cdots & b \\ \vdots & & \ddots & & \vdots \\ b & \cdots & b & a_{N-1} & b \\ b & b & \cdots & b & a_N + c \end{pmatrix}, \quad (7)$$

where

$$a_n = \frac{N-1}{\tilde{N}}\,k + k_0 - m_n\,\omega^2, \quad (8)$$

$$b = -\frac{k}{\tilde{N}}, \quad (9)$$

$$c = i\omega\gamma. \quad (10)$$

The inverse matrix $\hat{G} = \hat{Z}^{-1}$ is the Green's operator that provides the solution of the system of equations (2)–(4).

Actually, this is the particular solution for the initial condition $q_n = p_n = 0$ for all n. For long enough times, we expect the system to lose track of its initial configuration. This happens when masses are all different. In cases where this is not true, such as for equal masses, a full description of the motion of the particles should consider the role of the initial conditions. However, since this model is harmonic, the motion can always be seen as a superposition of the solutions caused by the interaction with the baths, which is stochastic, and the initial conditions, which are deterministic. Since our goal is to study the stochastic properties of the system, such as the heat flux, we will consider, even for equal masses, only the particular solution. We will see that our analytical results for equal masses remain valid for small mass heterogeneity.

III. RESULTS

The elements of the matrix $\hat{G} = \hat{Z}^{-1}$ can be obtained as

$$\hat{G}_{ij} = \hat{Z}^{-1}_{ij} = \frac{(-1)^{i+j}\hat{M}_{ij}}{\det(\hat{Z})}, \quad (11)$$

where $\det(\hat{Z})$ is the determinant of the matrix $\hat{Z}$ and $\hat{M}_{ij}$ is the (i, j) minor (i.e., the determinant of the submatrix that results from the elimination of the ith row and jth column of $\hat{Z}$). Derivations are essentially done through Laplace expansion of a determinant by minors.

For the modulus of the (i, j) minor, we straightforwardly obtain

$$|\hat{M}_{ij}| = \left| \frac{b}{A_i A_j} \prod_{n=1}^{N} A_n \right| \quad (12)$$

for $i \neq j$, where we have defined

$$A_i = a_i - b + c(\delta_{i1} + \delta_{iN}).$$

For $i = j$, the minor corresponds to the determinant of the matrix $\hat{Z}$ of reduced order.

The modulus of the determinant of the $N \times N$ matrix $\hat{Z}$ is

$$|\det(\hat{Z})| = \left| \left(1 + \sum_{j=1}^{N} \frac{b}{A_j}\right) \prod_{n=1}^{N} A_n \right|. \quad (13)$$

Then, for $i \neq j$,

$$|\hat{G}_{ij}| = \frac{|\hat{M}_{ij}|}{|\det(\hat{Z})|} = \left|\frac{A_i A_j}{b}\left(1 + \sum_{n=1}^{N} \frac{b}{A_n}\right)\right|^{-1}. \quad (14)$$

In the next sections, we will use the Green's operator $\hat{G}$ to find the heat flux and local temperature. Their mathematical expressions in terms of the elements of $\hat{G}$ are formally the same as previously derived in the literature for first-neighbor interactions (see, for instance, [49,50]), which are actually valid for any interaction network. In our case, the interactions are given by Eq. (7), where all off-diagonal elements are non-null due to the all-to-all interactions, in contrast to the tridiagonal first-neighbor case.

A. Transmittance and heat flux

In a long-range system, with all-to-all interactions, the bulk particle can receive heat through many channels, but we can calculate, without ambiguity, the fluxes that enter and leave the system [40], respectively, from the left bath to the first particle or from the rightmost particle to the right bath, which must coincide under stationary conditions, i.e.,

$$J = \langle(\eta_L - \gamma\dot{q}_1)\dot{q}_1\rangle = -\langle(\eta_R - \gamma\dot{q}_N)\dot{q}_N\rangle, \quad (15)$$

which has the form

$$J = \frac{T_L - T_R}{4\pi}\int_{-\infty}^{\infty} \mathcal{T}(\omega)d\omega, \quad (16)$$

where $\mathcal{T}(\omega)$ is the transmission coefficient,

$$\mathcal{T}(\omega) = 4\gamma^2\omega^2|\hat{G}_{1N}(\omega)|^2, \quad (17)$$

which depends on the bath properties (given only by γ in the case of our choice of baths) and on the system, via the element $\hat{G}_{1N}$, which can be obtained from Eq. (14).

Let us consider the particular case of identical masses, $m_n = m$, for all n. As we will discuss soon, this case yields normal modes uncoupled from the baths; however, the analytical results still apply in the limit of small heterogeneity in the masses, enough to recover the coupling with the baths.

From Eq. (14), we obtain

$$|\hat{G}_{1N}| = \frac{|b(a-b)|}{|a-b+c|\,|(a-b+Nb)(a-b+c) - 2cb|}. \quad (18)$$

Before continuing the mathematical derivation, it is insightful to analyze the eigenvectors of $\hat{Z}$ in Eq. (7) when masses are equal. Direct inspection of the matrix $\hat{Z}$, when $a_i = a$ for all i, allows us to identify that $\hat{q} = (1, 0, \ldots, 0, -1)$, corresponding to the relative motion of the end particles, is an eigenvector with eigenvalue $a - b + c$. Moreover, the vectors of the form $(0, \theta_2, \ldots, \theta_{N-1}, 0)$, subject to the constraint $\sum_{j=2}^{N-1}\theta_j = 0$, are eigenvectors with eigenvalue $a - b$. They span a subspace of dimension $N - 3$, corresponding to the relative motion of bulk particles and hence uncoupled to the baths. The two remaining eigenvectors have the form $\hat{q} = (1, \theta, \ldots, \theta, \ldots, \theta, 1)$, where θ can be obtained from $\hat{Z}\hat{q} = \lambda\hat{q}$, which allows us to identify the eigenvalues

$$\lambda^{\pm} = a + b + c + \theta^{\pm}b(N-2), \quad (19)$$

where

$$\theta^{\pm} = \frac{b(N-4) - c \pm \sqrt{[b(N-4)-c]^2 + 8b^2(N-2)}}{2b(N-2)}.$$

These modes are associated with rigid movements of the bulk. Finally, let us note that, if we multiply the eigenvalues to obtain the determinant and use Eq. (14), the eigenvalues of the modes uncoupled to the baths cancel out, and we recover Eq. (18). Substituting Eq. (18) into Eq. (17) and using the definitions of a, b, and c given by Eqs. (8), (9), and (10), we have

$$\mathcal{T}(\omega) = 4\gamma^2 w^2|\hat{G}_{1N}|^2 = 4\gamma^2 w^2\hat{G}_{1N}(\omega)\hat{G}_{1N}(-\omega) = \frac{4\gamma^2\omega^2k^2\left(\frac{Nk}{\tilde{N}} + k_0 - m\omega^2\right)^2}{f(\omega)\Delta(\omega)\tilde{N}^2}, \quad (20)$$

where

$$f(\omega) = \left(\frac{Nk}{\tilde{N}} + k_0 - m\omega^2\right)^2 + \gamma^2\omega^2, \quad (21)$$

$$\Delta(\omega) = \gamma^2\omega^2\left(\frac{2k}{\tilde{N}} + k_0 - m\omega^2\right)^2 + (k_0 - m\omega^2)^2\left(\frac{Nk}{\tilde{N}} + k_0 - m\omega^2\right)^2. \quad (22)$$

Let us remark that Eqs. (20)–(22) are valid for any $\tilde{N}$. We will analyze separately the momentum conserving ($k_0 = 0$) and nonconserving ($k_0 > 0$) systems. In the first case, mathematical expressions are common to both values of $\tilde{N}$; in the second, some expressions will be split for each value of $\tilde{N}$.

(i) When $k_0 = 0$, Eq. (20) reduces to

$$\mathcal{T}(\omega) = \frac{4\gamma^2k^2\left(\frac{Nk}{\tilde{N}} - m\omega^2\right)^2\frac{1}{\tilde{N}^2}}{f(\omega)\left[m^2\omega^2 f(\omega) - 4\gamma^2k\left(\frac{m\omega^2}{\tilde{N}} - \frac{k}{\tilde{N}^2}\right)\right]}, \quad (23)$$

where now $f(\omega) = (\frac{Nk}{\tilde{N}} - m\omega^2)^2 + \gamma^2\omega^2$. $\mathcal{T}(\omega)$ has an absolute maximum at $\omega = 0$. For $N^2/\tilde{N} \gg 4\gamma^2/(mk)$, only the maximum at $\omega = 0$ dominates (additional maxima with $\mathcal{T} < 1$ can emerge for small N). Therefore, for large enough N and $\omega^2 \ll Nk/(\tilde{N}m)$, Eq. (23) approaches

$$\mathcal{T}(\omega) \simeq \frac{1}{1 + N^2\left(\frac{m}{2\gamma}\right)^2\omega^2}, \quad (24)$$

which is a Lorentzian with a width that scales as $1/N$. This Lorentzian peak is associated with the complex conjugate pair of poles that get closer to the real axis when the dissipation parameter γ/m decreases. Equation (24) holds both with or without the Kac factor, and it is compared to exact results in Fig. 2.

Moreover, for large $\omega^2 \gg Nk/(\tilde{N}m)$, the transmittance decays as $\mathcal{T} \sim 1/(w^6\tilde{N}^2)$. This is depicted in the insets of Fig. 2 for the respective values of $\tilde{N}$. Hence, the integral in Eq. (16) is dominated by the Lorentzian peak described by Eq. (24), leading to

$$J/\Delta T \simeq \frac{\gamma/(2m)}{N}. \quad (25)$$

Furthermore, let us comment that, when the Kac factor is introduced, the behavior $\mathcal{T}(\omega) \sim 1/N^2$ is evident for any ω

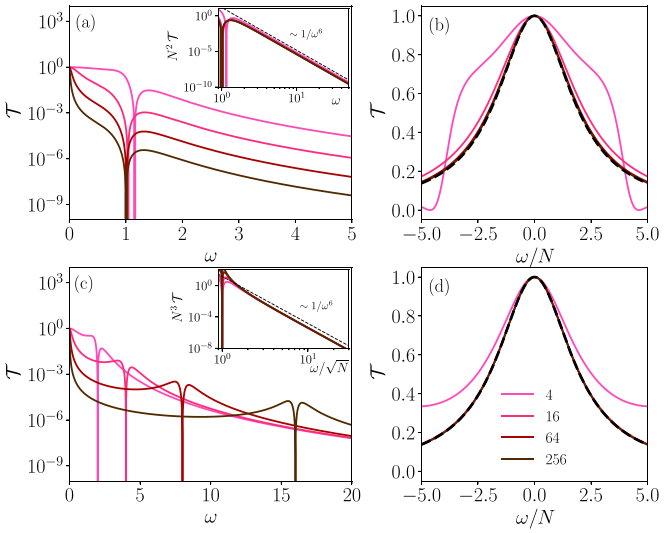

FIG. 2. Transmittance $\mathcal{T}(\omega)$ in the momentum conserving case (only the positive abscissa is displayed, keeping in mind that $\mathcal{T}$ is an even function) for the different values of N indicated in the legend (increasing N from lighter to darker) using Eq. (23). In all cases we used $m = k = \gamma = 1$ and $k_0 = 0$. In (a) and (b), $\tilde{N} = N - 1$, and in (c) and (d) $\tilde{N} = 1$. In (a)–(c), the insets highlight the scaling of the transmittance for large ω; the short-dashed lines correspond to the indicated power law, plotted as a reference. In (b) and (d), we focus on the main peak, and the black dashed lines correspond to the Lorentzian approximation given by Eq. (24), using the respective values of $\tilde{N}$.

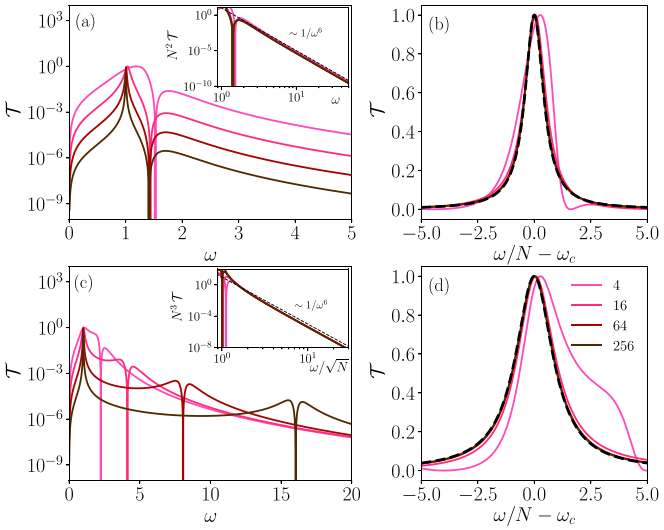

FIG. 3. Transmittance $\mathcal{T}(\omega)$ in the momentum nonconserving case with $k_0 = 1$. The remaining parameters are the same as in Fig. 2. For the Lorentzian approximation, Eqs. (28) and (29) were used, and ω_c is given by Eq. (26).

except in the global maxima where $\mathcal{T} = 1$ and in the zeros where $\mathcal{T} = 0$. If the Kac factor is eliminated, the same law does not hold for any frequency but still holds in the dominant region.

(ii) In the case $k_0 > 0$ (nonconserving), Eq. (23) takes the maximal value of 1 at frequencies $\pm\omega_c$, given by

$$\omega_c = \begin{cases} \omega_0 + \frac{\omega_0}{N}\frac{k\gamma^2/m}{k^2+\omega_0^2\gamma^2} + O(N^{-2}) & \text{if } \tilde{N} = N-1, \\ \omega_0 + O(N^{-2}) & \text{if } \tilde{N} = 1, \end{cases} \tag{26}$$

with $\omega_0 = \sqrt{k_0/m}$. These resonance frequencies can be obtained by solving $\mathcal{T}(\omega_c) = 1$, up to the first order of $1/N$. Other peaks are avoided for large enough N, verifying

$$\begin{aligned} N &\gg \frac{4k\gamma^2}{m}\frac{k^2-\omega_0^2\gamma^2}{\left(k^2+\omega_0^2\gamma^2\right)^2} && \text{if } \tilde{N} = N-1, \\ N^2 &\gg \frac{4\gamma^2}{mk} - \frac{2\omega_0^2\gamma^2}{k^2} && \text{if } \tilde{N} = 1. \end{aligned} \tag{27}$$

In such a case, the transmittance tends to the superposition of two Lorentzian peaks that narrow with increasing N (see Fig. 3) as

$$\mathcal{T}(\omega) \simeq \sum_{\Omega=\pm\omega_c} \frac{1}{1 + N^2\mathcal{A}^2(\omega-\Omega)^2}, \tag{28}$$

where

$$\mathcal{A} = \begin{cases} \frac{m}{\gamma}\left(1 + \frac{\omega_0^2\gamma^2}{k^2}\right) & \text{if } \tilde{N} = N-1, \\ \frac{m}{\gamma} & \text{if } \tilde{N} = 1. \end{cases} \tag{29}$$

The frequencies that significantly contribute to the transmission are those around $\pm\omega_c$, with bandwidths decreasing as $1/N$, which signals a localization [51,52]. Hence, also in this case

$$J/\Delta T \simeq \frac{1}{2\mathcal{A}N}. \tag{30}$$

This expression recovers Eq. (25) when $k_0 = 0$ and shows why when $\tilde{N} = 1$ the result does not depend on k_0, as observed in Fig. 4.

In conclusion, the flux decays as $1/N$. This result does not depend on the existence of pinning ($k_0 \neq 0$) or on the intro-

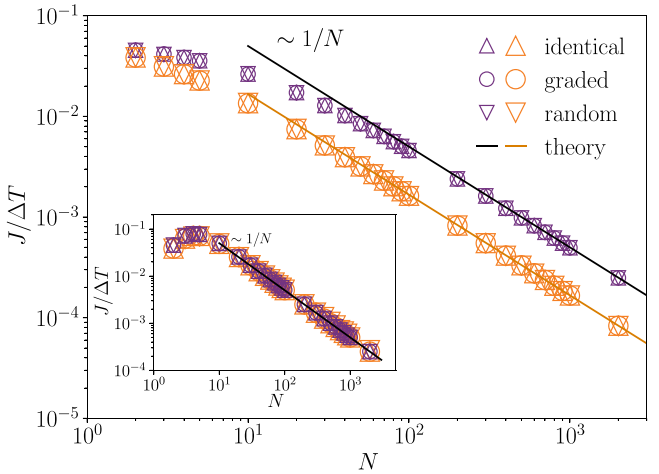

FIG. 4. Heat flux vs system size. The symbols correspond to the numerical integration of Eq. (17), while the solid lines correspond to the theoretical approximations valid for large N: Eq. (25) for $k_0 = 0$ and/or $\tilde{N} = 1$ and Eq. (30) otherwise. In all cases $\gamma = 1$, and $k = 0.1$, with $k_0 = 0$ (small dark purple symbols) or $k_0 = 0.02$ (large light orange symbols). In the main plot, we use $\tilde{N} = N - 1$, while in the inset $\tilde{N} = 1$ for the same values of the parameters. Besides identical masses $m = 1$, we also considered slightly graded and random distributions, with amplitude $\delta = 0.1$.

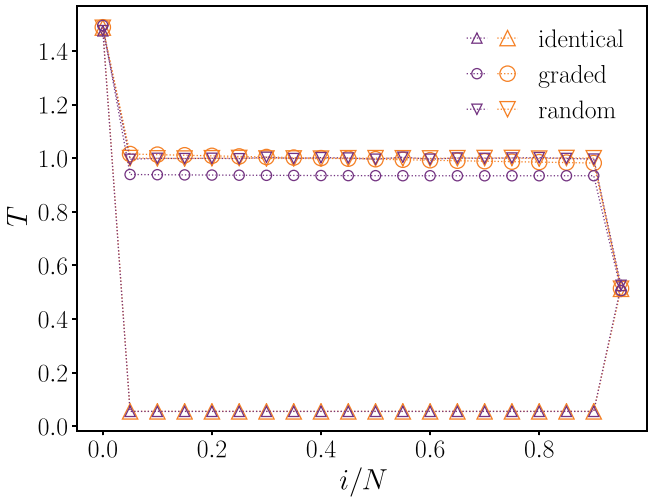

FIG. 5. Local temperature for the different configurations of masses indicated in the legend. In all cases, the average mass is $m = 1$. For random and graded masses, the amplitude is $\delta = 0.1$. We used $k = \gamma = 1$, $T_L = 1.5$, $T_R = 0.5$, and $N = 20$, with $k_0 = 0$ (large light orange symbols) or $k_0 = 1$ (small dark purple symbols). Symbols were obtained by performing the integration in Eq. (31) numerically. Lines are a guide to the eye. The results were obtained for $\tilde{N} = N - 1$ but are essentially the same for $\tilde{N} = 1$.

duction of a Kac factor. Such a scaling picture still holds when introducing a certain degree of heterogeneity in the masses. These effects are all illustrated in Fig. 4, where besides the case of identical masses developed analytically, we include numerical results by integrating Eq. (17) for other configurations of masses, with variations of small amplitude $\delta \ll 1$ around the average mass, namely, (i) graded masses, varying linearly between $m - \delta$ and $m + \delta$, that is, following the rule $m_n = m - \delta + 2\delta(n-1)/(N-1)$, and (ii) random masses, uniformly distributed in $[m - \delta, m + \delta]$. It is important to note that when all masses are distinct, symmetry breaking causes all modes to couple to baths, in contrast to the eigenmodes discussed above for equal masses, which is easy to see no longer applies. However, for small deviations from the average mass, the analytical expressions for the heat current, obtained for identical masses, still hold.

B. Local temperatures

The local temperature T_n, associated with the equilibrium position of particle n, is defined as two times its mean kinetic energy. According to the Green's function formalism, we have

$$T_n = m_n\langle(\dot{q}_n)^2\rangle = 2\gamma\, m_n \int_{-\infty}^{\infty} \frac{d\omega}{2\pi}\omega^2[T_L|\hat{G}_{n1}(\omega)|^2 + T_R|\hat{G}_{nN}(\omega)|^2]. \quad (31)$$

The minors and determinant required to obtain the elements $\hat{G}_{n1}$ and $\hat{G}_{nN}$ of the Green's operator were already defined in Eqs. (12) and (13), respectively.

In Fig. 5, we show the local temperatures as a function of the particle index, corresponding to the cases in Fig. 4, calculated by performing the integration in Eq. (31) numerically. By solving the stochastic equations of motion numerically, starting from particles at rest in their equilibrium positions, and averaging over many trials, we obtained results (not shown) consistent with those in Fig. 5.

The local temperature of the bulk is always nearly constant, but for the case of identical masses, the bulk does not thermalize. This is a consequence of the fact that only three eigenmodes are coupled to the baths: the one related to the relative motion of the end particles and two related to the rigid motion of the bulk. Meanwhile, due to the symmetry of the bulk particles, $N - 3$ normal modes are not coupled to the heat baths [47]. If this symmetry is suitably broken, even in a minimal way, all modes become coupled to the baths, hence enabling thermalization. This is what happens in the cases with graded or random masses shown in Fig. 5. In contrast, for instance, alternating masses (not shown) will not be enough.

In a very recent work, which also deals with the thermal problem in a very similar harmonic mean-field system, thermalization is achieved by introducing long-range couplings [53]. This means that off-diagonal terms in Eq. (7) become heterogeneous, while in our case heterogeneity is introduced in the diagonal of the inverse Green's operator.

Concerning the role of initial conditions, let us remark that the modes which are uncoupled to the bath will have sustained oscillations and therefore will not lose track of the initial conditions, while the modes coupled to the baths will be damped, hence forgetting the initial preparation. Therefore, although a system with homogeneous masses is anomalous in this respect, if all masses are different, the initial conditions will be irrelevant.

In all these cases, the temperature "profile" is nearly flat. When masses are equal, the level is of order $1/N$ and completely flat for the homogeneous initial conditions since all particles are equivalent. For subtly unequal masses, since the system thermalizes, the profile is around a level which corresponds to the average temperature. In the case of random masses there are small fluctuations. For a graded system, the temperature profile adopts a tilted shape, which can become very noticeable as the value of δ increases. However, this is artificial in the infinite-range case, where the spatial order of the bulk is lost and the transport between baths does not depend on the choice of which two particles are immersed in the baths.

IV. FINAL COMMENTS

We obtained exact expressions for the heat current and local temperature for systems of particles with arbitrary masses, coupled through a mean-field network of harmonic interactions.

For homogeneous masses, we obtained closed expressions. Although anomalous, in the sense that only a few modes are coupled to the baths and hence there is dependence on the initial conditions, the case of equal masses provides analytical results which represent an important reference for systems that do thermalize. As such, it is useful not only for the limit of incrementally unequal masses, as illustrated in Fig. 4, but also for sufficiently long range interactions, e.g., algebraically decaying with distance or with a fixed fraction of neighbors.

We can conclude that in the thermodynamic limit, the mean-field flux behaves as $J \sim 1/N$. This law is robust against

the existence of pinning or the introduction of a Kac factor. We verified (not shown) that the same scaling holds for a fixed boundary condition, i.e., setting $c = i\omega\gamma + k'$ in Eq. (10), which means that the end particles are harmonically linked (with stiffness k') to fixed ones. The observed scaling can be associated with the fact that the transmittance is dominated by one (conserving case) or two (nonconserving case) Lorentzian peaks with a width that decays as $1/N$. Let us note that nonoverlapping Lorentzian peaks were also observed in disordered harmonic chains with nearest-neighbor interactions in the weak and strong coupling limits [51].

We have seen that, for small deviations from the average mass, the analytical expressions for identical masses still hold. Differently, the $1/N$ law can be altered by disorder in the couplings if the Kac factor is not used, in which case the current becomes constant for large N [47]. This is observed when the Kac factor is not used, i.e., when $\tilde{N} = 1$. In fact, in such a case, a band whose integral does not depend on N appears in the transmittance and hence dominates over the contribution of the peak that we observe in the absence of stiffness disorder, even for a low amplitude of the fluctuations. We also noticed that when the Kac factor is introduced, the contribution of this band decreases as $1/N$; hence, the heat current does too.

Regarding the local temperatures, similar to the nearest-neighbor case, the bulk temperature is nearly uniform, but the level corresponding to the average of the baths is attained only for some scattering component even if it is perturbative.

For comparison, let us recall that, for nearest neighbors, mass-gradient harmonic chains [54,55], as well as identical masses, produce a constant current. In (stiffness) disordered chains with nearest-neighbor interactions, it has been reported that, when disorder has a heavy-tailed distribution, the current scales as $1/N$ [51]. In the mean-field case, although the current scales as $1/N$, the concept of conductivity and hence Fourier law does not apply properly. Despite this limitation, the mean-field model for equal masses is still a useful tool as it allows clear analytical results which remain valid even for different masses where the bulk particles thermalize. Notice, however, that for graded and random masses, despite thermalization, the flat temperature profile indicates the breakdown of Fourier's law.

Let us also remark that since the system is harmonic, it can be decomposed into N normal modes; then the energy is always extensive, but for all-to-all interactions without a Kac factor, the entropy is not extensive, and frequency grows with $\sqrt{N}$. If we eliminate the Kac factor by setting $\tilde{N} = 1$ in Eq. (1) and hence in Eq. (9), we note that Eq. (24) remains valid, as does Eq. (28), implying that the results for the scaling of the heat current are not altered by the use or lack of the Kac factor in the mean-field model.

As a natural extension of this work, it would be interesting to obtain analytical results for a finite range of the interactions, decaying algebraically with the interparticle distance. In this case the chain order would be recovered, and the transition between the first-neighbor and mean-field limits would be accessed.

ACKNOWLEDGMENTS

C.O. gratefully acknowledges enlightening discussions with A. Dhar and S. Lepri. C.A. acknowledges partial financial support from the Brazilian agencies CNPq (Grant No. 311435/2020-3) and FAPERJ (Grant No. CNE E-26/201.109/2021). CAPES (code 001) is also acknowledged.

[1] S. Lepri, R. Livi, and A. Politi, Phys. Rep. **377**, 1 (2003).
[2] A. Dhar, Adv. Phys. **57**, 457 (2008).
[3] S. Lepri, R. Livi, and A. Politi, in *Thermal Transport in Low Dimensions: From Statistical Physics to Nanoscale Heat Transfer*, edited by S. Lepri (Springer, Heidelberg, 2016), Chap. 1, pp. 1–37.
[4] G. Benenti, S. Lepri, and R. Livi, Front. Phys. **8**, 292 (2020).
[5] F. Bonetto, J. L. Lebowitz, and L. Rey-Bellet, Math. Phys. **2000**, 128 (2000).
[6] O. Narayan and S. Ramaswamy, Phys. Rev. Lett. **89**, 200601 (2002).
[7] G. T. Landi and M. J. de Oliveira, Phys. Rev. E **89**, 022105 (2014).
[8] Y. Li, S. Liu, N. Li, P. Hänggi, and B. Li, New J. Phys. **17**, 043064 (2015).
[9] S. Liu, P. Hänggi, N. Li, J. Ren, and B. Li, Phys. Rev. Lett. **112**, 040601 (2014).
[10] S. G. Das and A. Dhar, arXiv:1411.5247 [cond-mat.stat-mech].
[11] C. Giardiná, R. Livi, A. Politi, and M. Vassalli, Phys. Rev. Lett. **84**, 2144 (2000).
[12] C. W. Chang, D. Okawa, H. Garcia, A. Majumdar, and A. Zettl, Phys. Rev. Lett. **101**, 075903 (2008).
[13] N. Yang, G. Zhang, and B. Li, Nano Today **5**, 85 (2010).
[14] Z. Wang, J. A. Carter, A. Lagutchev, Y. K. Koh, N.-H. Seong, D. G. Cahill, and D. D. Dlott, Science **317**, 787 (2007).
[15] T. Meier, F. Menges, P. Nirmalraj, H. Hölscher, H. Riel, and B. Gotsmann, Phys. Rev. Lett. **113**, 060801 (2014).
[16] C.-W. Chang, in *Experimental Probing of Non-Fourier Thermal Conductors* (eds.) S. Lepri, Thermal Transport in Low Dimensions. Lecture Notes in Physics, Vol. 921 (Springer, Cham, 2016), pp. 305–338.
[17] N. Li, J. Ren, L. Wang, G. Zhang, P. Hänggi, and B. Li, Rev. Mod. Phys. **84**, 1045 (2012).
[18] C. W. Chang, D. Okawa, A. Majumdar, and A. Zettl, Science **314**, 1121 (2006).
[19] B. Li, L. Wang, and G. Casati, Phys. Rev. Lett. **93**, 184301 (2004).
[20] E. Pereira, Phys. Rev. E **96**, 012114 (2017).
[21] E. Pereira and R. R. Ávila, Phys. Rev. E **88**, 032139 (2013).
[22] S. Chen, E. Pereira, and G. Casati, Europhys. Lett. **111**, 30004 (2015).
[23] A. Campa, T. Dauxois, and S. Ruffo, Phys. Rep. **480**, 57 (2009).
[24] Y. Levin, R. Pakter, F. B. Rizzato, T. N. Teles, and F. P. Benetti, Phys. Rep. **535**, 1 (2014).
[25] S. Gupta and S. Ruffo, Int. J. Mod. Phys. A **32**, 1741018 (2017).
[26] *Dynamics and Thermodynamics of Systems with Long Range Interactions*, edited by T. Dauxois, S. Ruffo, E. Arimondo, and M. Wilkens (Springer, Berlin, 2002).
[27] J. Barré, D. Mukamel, and S. Ruffo, Phys. Rev. Lett. **87**, 030601 (2001).

[28] F. A. Tamarit and C. Anteneodo, Phys. Rev. Lett. **84**, 208 (2000).
[29] A. Campa, A. Giansanti, and D. Moroni, Phys. Rev. E **62**, 303 (2000).
[30] C. Anteneodo, Phys. A (Amsterdam, Neth.) **342**, 112 (2004).
[31] T. M. Rocha Filho, M. A. Amato, B. A. Mello, and A. Figueiredo, Phys. Rev. E **84**, 041121 (2011).
[32] M. Antoni and S. Ruffo, Phys. Rev. E **52**, 2361 (1995).
[33] V. Latora, A. Rapisarda, and C. Tsallis, Phys. Rev. E **64**, 056134 (2001).
[34] D. Mukamel, S. Ruffo, and N. Schreiber, Phys. Rev. Lett. **95**, 240604 (2005).
[35] L. G. Moyano and C. Anteneodo, Phys. Rev. E **74**, 021118 (2006).
[36] T. M. Rocha Filho, M. A. Amato, A. E. Santana, A. Figueiredo, and J. R. Steiner, Phys. Rev. E **89**, 032116 (2014).
[37] C. Olivares and C. Anteneodo, Phys. Rev. E **94**, 042117 (2016).
[38] D. Bagchi and C. Tsallis, Phys. Lett. A **381**, 1123 (2017).
[39] D. Bagchi, Phys. Rev. E **95**, 032102 (2017).
[40] S. Iubini, P. Di Cintio, S. Lepri, R. Livi, and L. Casetti, Phys. Rev. E **97**, 032102 (2018).
[41] P. Di Cintio, S. Iubini, S. Lepri, and R. Livi, J. Phys. A. **52**, 274001 (2019).
[42] R. Livi, J. Stat. Mech. (2020) 034001.
[43] D. Bagchi, Phys. Rev. E **96**, 042121 (2017).
[44] J. Wang, S. V. Dmitriev, and D. Xiong, Phys. Rev. Research **2**, 013179 (2020).
[45] D. Bagchi, Phys. Rev. E **104**, 054108 (2021).
[46] S. Tamaki and K. Saito, Phys. Rev. E **101**, 042118 (2020).
[47] M. Schmidt, T. Kottos, and B. Shapiro, Phys. Rev. E **88**, 022126 (2013).
[48] M. Kac, G. E. Uhlenbeck, and P. C. Hemmer, J. Math. Phys. **4**, 216 (1963).
[49] A. Dhar, Phys. Rev. Lett. **86**, 5882 (2001).
[50] A. Dhar and R. Dandekar, Phys. A (Amsterdam, Neth.) **418**, 49 (2015).
[51] B. Ash, A. Amir, Y. Bar-Sinai, Y. Oreg, and Y. Imry, Phys. Rev. B **101**, 121403(R) (2020).
[52] G. Cane, J. Majeed Bhat, A. Dhar, and C. Bernardin, J. Stat. Mech. (2021) 113204.
[53] F. Andreucci, S. Lepri, S. Ruffo, and A. Trombettoni, arXiv:2112.11580.
[54] K. V. Reich, Phys. Rev. E **87**, 052109 (2013).
[55] N. Yang, N. Li, L. Wang, and B. Li, Phys. Rev. B **76**, 020301(R) (2007).